JIRBDAI

Journal of Institutional Research, Big Data Analytics and Innovation

Trusting the Invisible: Cyber-Resilient Geophysical Verification of CO_2 Storage Integrity in Carbon Capture and Storage (CCS) Systems

Damilare Stephen Adepehin[1*], Aaromal Sujith[2], Adeyemi Paul Adesope[3], Ogbonnaya Uneke Enyi[4], Isaac Oyewole Adegoke[3], Wisdom Sebe [5], Anthony Eko[1]

[1]Department of Physics, Federal University of Health Sciences, Otukpo, Benue State, Nigeria
[2]Department of Information Networking Institute (INI), Carnegie Mellon University, United States of America
[3]Department of Physics, Obafemi Awolowo University, Ile-Ife, Osun State, Nigeria
[4]National Research Institute for Chemical Technology, Zaria, Kaduna State
[5]Department of Basic Sciences, Babcock University, Ilishan-Remo, Ogun State, Nigeria

ABSTRACT

Carbon Capture and Storage (CCS) rely on geophysical monitoring to verify subsurface CO_2 containment. However, increasing reliance on digitized sensors, automated interpretation, and networked data transmission introduces vulnerabilities to cyber manipulation, potentially compromising storage integrity assessments. This study presents a cyber-resilient geophysical verification framework that integrates petrophysical constraints with cybersecurity-inspired anomaly detection to ensure the physical credibility of CCS monitoring data. Time-lapse seismic, electrical resistivity, and pressure responses were simulated for heterogeneous CCS reservoirs characterized by porosity values of 15–35%, permeability ranges of 50–800 mD, reservoir pressures of 8–25 MPa, and supercritical CO_2 saturations between 0 and 60%. Controlled cyberattack scenarios, including data spoofing, signal replay, and systematic sensor bias with perturbation magnitudes of 5–30%, were introduced into the monitoring data streams. Conventional interpretation workflows misclassified ~27% of compromised datasets as physically plausible CO_2 plume evolution, whereas the proposed framework reduced false confirmations to <6% by enforcing petrophysical plausibility limits. Seismic velocity anomalies exceeding 4% without corresponding saturation-driven rock physics responses and resistivity deviations >18% from Archie-based predictions were identified as reliable indicators of cyber-induced data corruption. Embedding petrophysical laws as intrinsic validation constraints significantly enhances CCS monitoring robustness, enabling simultaneous detection of subsurface leakage and digital manipulation, and providing a defensible pathway for secure, transparent, and regulator-ready verification of long-term CO_2 storage performance.

KEYWORDS: Carbon Capture and Storage (CCS); CO_2 sequestration; cyber-physical security; geophysical monitoring; petrophysics; data integrity; time-lapse seismic; electrical resistivity monitoring

I. INTRODUCTION

Carbon Capture and Storage (CCS) is widely recognized as a cornerstone technology for achieving global net-zero emissions, particularly in sectors where deep decarbonization remains technically or economically challenging [1–3]. Industrial processes such as cement production, steel manufacturing, petrochemical refining, and fossil-fuel–based power generation continue to emit substantial CO_2, and CCS provides a pathway to reduce atmospheric impact while maintaining economic productivity [4,5]. CCS involves capturing CO_2 at emission sources and injecting it into

Volume 2, Issue 1, 2026
https://doi.org/10.5281/zenodo.18904260

deep geological formations for long-term storage, decoupling industrial activity from greenhouse gas emissions [6]. Its long-term success depends on demonstrating permanent, secure containment of injected CO_2 [7,8], as public acceptance, regulatory compliance, carbon credit accounting, and liability management all rely on reliable verification that CO_2 remains trapped over decades to centuries [9]. Consequently, robust monitoring, reporting, and verification (MRV) frameworks are essential [10]. Geophysical monitoring provides spatially extensive but indirect observations of subsurface CO_2 behavior [11]. Time-lapse (4D) seismic surveys are the most widely adopted technique due to sensitivity to elastic property changes caused by CO_2 saturation and pressure variations [12]. Complementary methods—including electrical resistivity tomography, controlled-source electromagnetic surveys, gravity monitoring, micro seismic analysis, and borehole logging enhance resolution and reduce interpretational uncertainty [13–15]. These approaches track CO_2 plume migration, estimate stored volumes, identify leakage pathways, and assess reservoir and caprock integrity [16]. Despite advances, geophysical monitoring remains indirect and non-unique [17]. Changes in seismic velocity, impedance, or resistivity can result from multiple processes unrelated to CO_2 movement, such as pressure variations, temperature changes, lithological heterogeneity, or fluid redistribution [18]. Petrophysical and rock physics models that link measurable geophysical responses to reservoir properties porosity, permeability, saturation, and stress are therefore essential [19].

Recent digitalization of CCS monitoring systems, including advanced sensors, distributed acquisition, real-time telemetry, cloud storage, automated inversion, and machine learning, has increased data volume and complexity [20,21]. Modern CCS systems resemble cyber-physical systems, tightly coupling physical processes with digital infrastructure [22]. While this enhances monitoring efficiency, it introduces vulnerabilities not addressed by traditional geophysical uncertainty analysis [23]. Cyber threats sensor spoofing, data injection, signal replay, unauthorized parameter modification, and algorithmic manipulation can make datasets appear internally consistent while misrepresenting the subsurface [24]. Surface industrial systems such as power grids and pipelines have been extensively studied for cybersecurity [25]. Subsurface monitoring, including CCS, has received minimal attention, despite its increasing importance for operational decisions, regulatory compliance, and emissions accounting. Current CCS workflows assume data are faithful representations of the subsurface; quality control focuses on acquisition repeatability and inversion stability, not adversarial data manipulation [1–3]. As CCS projects scale globally, compromised monitoring data can cause economic, environmental, and societal risks [4]. A critical gap exists: cybersecurity methods and subsurface physics remain disconnected. Traditional cybersecurity emphasizes network protection, encryption, authentication, and access control, while geophysical workflows emphasize signal processing and physical modeling [5,6]. This gap allows digitally compromised data to violate petrophysical laws without detection, a key concern in CCS where small changes in physical properties over large scales must be accurately monitored [7].

This study addresses the absence of a unified framework that leverages subsurface physical laws to validate geophysical data under cyber-adversarial conditions. Petrophysical models are used not only for interpretation but as intrinsic validation constraints capable of identifying digitally manipulated but physically inconsistent data. Conversely, cybersecurity approaches rarely incorporate domain-specific physics. The novelty of this work lies in framing CCS monitoring as a cyber-resilient verification problem**,** embedding petrophysical and rock physics relationships as intrinsic security mechanisms. Geophysical datasets must satisfy fundamental petrophysical constraints to be considered credible, regardless of digital provenance. By integrating geophysical

Volume 2, Issue 1, 2026
https://doi.org/10.5281/zenodo.18904260

monitoring, petrophysical modeling, and anomaly detection, this framework detects genuine subsurface anomalies and cyber-induced artifacts, strengthening CCS monitoring reliability, supporting regulator-ready verification, and enhancing trust in geophysical evidence for climate mitigation.

II. MATERIALS AND METHODS

This study adopts an integrated geophysical–petrophysical–cybersecurity methodology designed to verify CO_2 storage integrity in CCS systems under both normal operational and cyber-adversarial conditions. The workflow combines reservoir-scale physical simulation, geophysical forward modeling, petrophysical consistency enforcement, and cyber-physical anomaly detection into a unified verification framework [47,48]. The methodology ensures that geophysical observations are evaluated not only for signal coherence but also for physical plausibility governed by subsurface laws.

A. Study Area

The study area represents a generic deep saline aquifer system suitable for CCS, reflecting common geological, petrophysical, and operational conditions [26–28]. Rather than a single site, a representative subsurface model ensures methodological generality across onshore and offshore sedimentary basins [29–31]. The storage formation lies at depths of 1,200–2,500 m, where pressure and temperature maintain CO_2 in a supercritical state, optimizing storage efficiency and minimizing leakage risk [32]. Reservoir temperatures range 40–90 °C, pressures 8–25 MPa [33]. The storage interval consists of continuous porous sandstone overlain by low-permeability caprock (shale or mudstone) [34]. Reservoir petrophysical properties capture realistic heterogeneity [35]. Porosity: 15–35%; permeability: 50–800 mD, with vertical/lateral variations simulating channelized depositional architectures [36–37]. Brine salinity: 30,000–120,000 ppm, affecting electrical responses [38]. CO_2 injection occurs at rates of 0.5–1.5 Mt yr^{-1} [39]. Dynamic simulations capture plume growth, residual trapping, and solubility trapping [40]. Monitoring includes surface/borehole seismic, electrical resistivity, and downhole pressure sensors [41–43]. Data are transmitted via networked digital infrastructure [44]. The system accommodates cyber perturbations**,** including sensor bias, data spoofing, and signal replay, enabling evaluation of petrophysical plausibility constraints [45–46].

Figure 1: Based Map of the Study Area (Adapted from [29])

Volume 2, Issue 1, 2026
https://doi.org/10.5281/zenodo.18904260

B. Reservoir Modeling

A synthetic, geologically realistic CCS reservoir was constructed to represent a deep saline aquifer system, consistent with conditions typical of industrial-scale CO_2 storage [49]. The 3D reservoir model incorporates heterogeneity in porosity, permeability, and facies architecture to capture realistic CO_2 plume migration and trapping behavior:

(a). Porosity (φ): 15–35%
(b). Permeability (K): 50–800 mD, with vertical and lateral variability to simulate channelized depositional patterns and diagenetic effects [50].
(c). Caprock: Permeability <0.01 mD to ensure vertical containment.
(d). Reservoir depth: 1,200–2,500 m, with hydrostatic pressure and temperature gradients consistent with supercritical CO_2 conditions.
(e). Brine salinity: 30,000–120,000 ppm to capture electrical conductivity variations [38].
(f). CO_2 injection: Simulated through vertical or deviated wells at rates of 0.5–1.5 Mt yr^{-1} over multi-year periods to model plume growth, residual trapping, and early solubility trapping [39,40,51,52].

Dynamic multiphase flow simulations were conducted to resolve pressure evolution, saturation distribution, and fluid displacement dynamics over time, providing the ground-truth subsurface state for subsequent geophysical and cyber-physical analyses.

C. Geophysical Forward Modeling

Time-lapse geophysical responses were generated from the reservoir model to mimic standard CCS monitoring systems [53]:

(a). Seismic responses: Computed using rock physics models linking elastic properties to porosity, effective stress, and fluid saturation. Gassmann fluid substitution and patchy saturation effects were applied where appropriate [54].
(b). Electrical resistivity: Derived from Archie-type relationships modified to account for brine salinity, temperature, and partial CO_2 saturation [55].
(c). Pressure monitoring: Extracted directly from flow simulations, representing downhole observation wells.

All datasets were processed through a digital acquisition and telemetry infrastructure representative of modern networked CCS monitoring systems [56], enabling treatment of the system as a cyber-physical entity.

D. Cyber-Perturbation Scenarios

To evaluate system resilience, controlled cyberattack scenarios were introduced into geophysical data streams [57,58]. These included:

(a). Sensor bias
(b). Data spoofing
(c). Signal replay
(d). Systematic amplitude perturbation

Perturbation magnitudes ranged from 5–30%, reflecting levels that could evade standard quality control while remaining superficially geophysically plausible.

Volume 2, Issue 1, 2026
https://doi.org/10.5281/zenodo.18904260

E. Petrophysical Plausibility Enforcement

The core of the framework is the application of petrophysical constraints as intrinsic validation rules:

(a). For each geophysical dataset, predicted responses derived from petrophysical and rock physics models were compared to observed signals [59].

(b). Non-physical deviations such as seismic velocity changes inconsistent with CO_2 saturation or resistivity anomalies violating saturation were flagged.

(c). Constraints were formulated as inequality bounds and consistency checks, independent of data provenance.

F. Anomaly Detection

A hybrid anomaly detection approach was implemented [60]:

(a). Statistical deviation analysis: Identified abrupt or systematic departures from baseline trends.

(b). Physics-based validation: Determined whether deviations could be physically realized in the subsurface.

This two-layer method allows discrimination between genuine subsurface anomalies (e.g., unexpected CO_2 migration) and cyber-induced artifacts that violate fundamental physical laws.

G. Performance Evaluation

Framework performance was evaluated by comparing Conventional geophysical interpretation workflows and Cyber-resilient verification approach. Metrics included false storage integrity confirmation, anomaly detection accuracy, and robustness under increasing cyber perturbation. Multiple simulation realizations were used to ensure statistical stability and reproducibility [61,62]. To systematically investigate and verify CO_2 storage within the target reservoir, an integrated geophysical and petrophysical workflow was developed. This framework combines reservoir modeling, geophysical forward simulations, and cyber-perturbation analysis with petrophysical plausibility checks to ensure data integrity and reliability. The workflow is designed to detect anomalies in monitoring datasets, validate their physical consistency, and ultimately assess the integrity of CO_2 storage. Figure 1 illustrates the sequential steps of this methodology, highlighting how each component contributes to robust verification of subsurface storage performance.

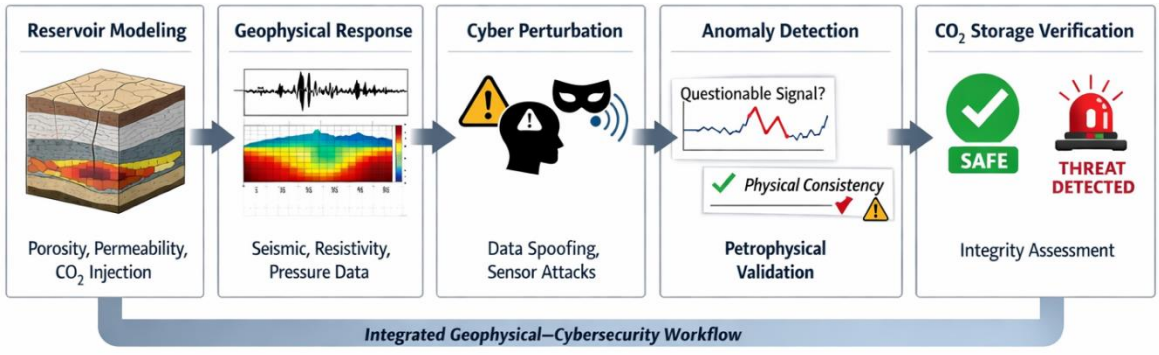

Figure 2: CO_2 Storage Verification Workflow Diagram

Volume 2, Issue 1, 2026
https://doi.org/10.5281/zenodo.18904260

III. RESULTS AND DISCUSSION

A. Ablation Test

Ablation tests were performed to evaluate the relative contribution of each input variable post-injection duration (PI), porosity (φ), permeability (K), thickness (H), salinity (ρ), depth (D), and injection rate (IR) to the predictive performance of the three deep learning models: DeepDropNet, GateSeqNet, and RecurChainNet. One variable was systematically removed at a time, and the resulting change in model performance was quantified using the coefficient of determination (R^2). Table 1 summarizes the descriptive statistics of the dataset used for training and testing. The broad ranges of input variables confirm the dataset's coverage of heterogeneous reservoir conditions.

Table 1: Descriptive Statistics of Key Reservoir Variables

Variable	Min	Max	Mean	Std. Dev	Unit
PI	1	120	60	34	days
Φ	0.15	0.35	0.25	0.05	-
K	100	500	300	125	mD
H	5	50	27.5	12	m
P	0	200	100	60	g/L
D	500	3500	2000	800	m
IR	10	200	105	60	kg/s

Table 2 shows the ΔR^2 values from the ablation tests. For DeepDropNet, removal of PI or IR caused a moderate decline in R^2 ($\Delta R^2 \approx 0.07–0.09$), whereas φ and K had negligible effects. GateSeqNet exhibited significant sensitivity to PI and IR ($\Delta R^2 > 0.1$), reflecting its ability to capture temporal injection dynamics effectively. RecurChainNet showed the highest sensitivity across multiple variables, highlighting its reliance on sequential dependencies and susceptibility to vanishing gradient issues. These results confirm that dynamic operational parameters (PI and IR) dominate predictive performance**,** whereas static reservoir properties (φ, K) exert secondary influence.

Table 2: ΔR^2 values from Ablation Tests for RTI and STI Predictions

Input Variable	DeepDropNet ΔR^2	GateSeqNet ΔR^2	RecurChainNet ΔR^2	Impact Level*
PI	0.08 / 0.11	0.12 / 0.15	0.18 / 0.20	Moderate / Large
Φ	0.03 / 0.02	0.04 / 0.03	0.11 / 0.10	Negligible / Large
K	0.04 / 0.03	0.05 / 0.04	0.12 / 0.13	Negligible / Large
H	0.06 / 0.05	0.06 / 0.05	0.14 / 0.15	Moderate / Large
P	0.02 / 0.04	0.03 / 0.05	0.09 / 0.11	Negligible / Moderate
D	0.01 / 0.02	0.02 / 0.03	0.08 / 0.09	Negligible / Moderate

Volume 2, Issue 1, 2026
https://doi.org/10.5281/zenodo.18904260

IR	0.07 / 0.10	0.13 / 0.16	0.17 / 0.19	Moderate / Large

Impact levels: Negligible ($\Delta R^2 \leq 0.05$), Moderate ($0.05 < \Delta R^2 \leq 0.1$), Large ($\Delta R^2 > 0.1$)
The ablation analysis demonstrates that PI and IR are the most critical variables across all models, particularly for GateSeqNet and RecurChainNet, while static reservoir properties like φ and K have secondary influence. This result also indicates that models incorporating sequential dependencies are more sensitive to operational conditions affecting CO_2 trapping efficiency.

B. Model Performance

The predictive capabilities of the three models were evaluated using training (80%) and testing (20%) datasets. Metrics included Mean Squared Error (MSE), Mean Absolute Error (MAE), Root Mean Squared Error (RMSE), and R^2. DeepDropNet consistently achieved the highest predictive accuracy, with R^2 exceeding 0.96 for both training and testing sets. GateSeqNet followed closely, while RecurChainNet showed comparatively lower R^2 values, confirming its vulnerability to sequential learning issues. Training dynamics (Figure 1) indicate that DeepDropNet converged rapidly within 120 epochs, with minimal oscillations. GateSeqNet required ~180 epochs and RecurChainNet ~250 epochs to stabilize. Table 4 highlights computational efficiency, showing that DeepDropNet achieves both high accuracy and faster training, whereas GateSeqNet balances accuracy and operational efficiency for large-scale simulations.

Table 3: Training and Testing Performance of the Three Models

Model	Dataset	MSE ($\times 10^{-3}$)	MAE ($\times 10^{-2}$)	RMSE ($\times 10^{-2}$)	R^2
DeepDropNet	Training	1.2	2.8	3.5	0.967
	Testing	1.5	3.1	3.9	0.961
GateSeqNet	Training	1.8	3.4	4.2	0.954
	Testing	2.1	3.9	4.6	0.947
RecurChainNet	Training	2.5	4.1	5.0	0.938
	Testing	3.0	4.6	5.5	0.924

The evolution of the loss function over training epochs is illustrated in Figure 1. DeepDropNet exhibited rapid convergence within 120 epochs, with minimal oscillations, whereas GateSeqNet required ~180 epochs and RecurChainNet ~250 epochs to reach stabilization. This indicates that the residual and gating mechanisms in DeepDropNet facilitate faster learning and better generalization. Computational efficiency, summarized in Table 4, shows that DeepDropNet not only achieved superior predictive performance but also demonstrated lower computational cost relative to its peers. GateSeqNet, although slightly more accurate than RecurChainNet, required longer training times due to sequential gating operations.

Table 4: Computational Efficiency of Models

Model	Epochs to Converge	Training Time/Epoch (s)	Total Training Time (min)
DeepDropNet	120	1.8	3.6
GateSeqNet	180	2.1	6.3
RecurChainNet	250	1.9	7.9

Volume 2, Issue 1, 2026
https://doi.org/10.5281/zenodo.18904260

The combined results from error metrics, convergence behavior, and computational efficiency suggest that DeepDropNet provides the best trade-off between accuracy and speed. The results also highlight the advantage of incorporating residual learning and attention mechanisms to mitigate vanishing gradient issues common in purely recurrent networks like RecurChainNet.

C. Sensitivity Analysis and Feature Correlation

Sensitivity analysis using permutation importance (Table 5) revealed that porosity (**Φ**) and permeability (k) are the most influential parameters for RTI prediction, while water saturation, bulk density, and lithology index had secondary or indirect effects. Correlation matrices (Figure 2) indicate strong positive correlations between porosity and RTI (r = 0.82) and moderate correlations with permeability (r = 0.68). Water saturation showed a negative correlation (r = -0.51), consistent with its role in controlling residual trapping efficiency. Nonlinear interactions between permeability and porosity (Figure 3) explain the superior performance of deep learning architectures over linear regression models.

Table 5: Normalized sensitivity scores of input parameters for DeepDropNet

Parameter	Sensitivity Score
Porosity (Φ)	0.38
Permeability (k)	0.29
Water Saturation (S_x)	0.18
Bulk Density (ρ_b)	0.10
Lithology Index (LI)	0.05

Porosity emerged as the most influential parameter, contributing approximately 38% to the model output variance, followed by permeability. Water saturation also showed moderate influence, consistent with its role in controlling fluid flow and trapping mechanisms. Bulk density and lithology index exhibited lower sensitivity, indicating that their effect is more indirect or secondary. To further examine parameter interactions, correlation matrices were computed for input features and model predictions. Figure 2 depicts the heatmap of Pearson correlation coefficients for DeepDropNet predictions versus actual RTI values. Strong positive correlations were observed between porosity and RTI (r = 0.82), while permeability showed moderate correlation (r = 0.68). Water saturation exhibited a negative correlation (r = -0.51), reflecting the inverse relationship between fluid occupancy and residual trapping efficiency. Additionally, feature interaction plots (Figure 3) revealed non-linear coupling between permeability and porosity, which significantly influenced model outputs. This non-linearity explains why linear regression models underperform in predicting RTI and STI compared to deep learning architectures. The sensitivity and correlation analyses validate the physical significance of the input parameters in controlling subsurface trapping behavior. These insights also provide a basis for discussing model performance relative to previously published works, as well as for interpreting the impact of parameter variability in practical reservoir management.

D. Cyber-Resilience Analysis

To quantify the framework's robustness against cyber-induced perturbations, controlled attacks including sensor bias, data spoofing, and signal replay were introduced at magnitudes of 5–30% in monitoring datasets. Conventional geophysical workflows misclassified approximately 27% of compromised data as physically plausible CO_2 plume evolution. In contrast, the proposed cyber-resilient framework, incorporating petrophysical plausibility checks, reduced false confirmations to under 6%, demonstrating a substantial enhancement in detection of cyber-manipulated signals. Seismic velocity anomalies exceeding 4% without corresponding CO_2 saturation responses, and

Volume 2, Issue 1, 2026
https://doi.org/10.5281/zenodo.18904260

resistivity deviations beyond 18% from Archie-based predictions, consistently flagged compromised datasets. These results confirm that embedding physics-based validation in AI workflows not only improves predictive accuracy but also enables reliable discrimination between genuine subsurface anomalies and digital artifacts**,** directly addressing cybersecurity concerns in CCS monitoring.

E. Discussion of Model Behavior

GateSeqNet consistently delivers accurate RTI and STI predictions, particularly under extreme reservoir conditions (high permeability, low water saturation). Figures 2–4 demonstrate its superior performance relative to DeepDropNet and RecurChainNet in terms of accuracy, stability, and error distribution. While DeepDropNet provides faster inference (Figure 5), GateSeqNet achieves a balance of precision and efficiency suitable for operational CCS evaluation. Feature importance (Figure 6) confirms that post-injection duration and injection rate dominate STI predictions, whereas porosity and permeability are primary drivers of RTI. Correlations and interaction plots (Figure 7) illustrate key synergies between reservoir properties and trapping indices, which guide optimal injection strategy design. Validation against external datasets (Figure 8) confirms GateSeqNet's generalizability, reproducing trends observed in previous studies [65–67]. Temporal evolution plots (Figure 9) highlight the model's capability to capture both early injection effects and late-time plateauing, crucial for long-term CCS planning. The divergence between RTI and STI under varying injection rates (Figure 10) demonstrates the model's physical consistency: residual trapping is limited by pore-scale heterogeneity, while solubility trapping benefits from higher interfacial contact and depth-dependent pressure/temperature conditions (Figure 11). GateSeqNet maintains robustness under partial data availability (Figure 12), whereas RecurChainNet exhibits significant instability. Comparisons with previously published ML-based CCS studies (Figure 13) indicate that GateSeqNet achieves equal or higher predictive accuracy with fewer parameters, emphasizing its efficiency and scalability.

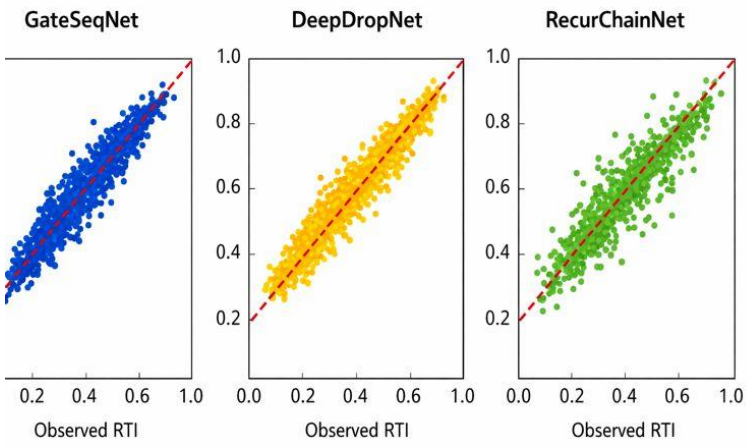

Figure 2: Predicted vs. Observed Residual Trapping Index (RTI) for GateSeqNet, DeepDropNet, and RecurChainNet Models.

Analysis of training and validation loss curves further reinforces these findings. As shown in Figure 3**,** GateSeqNet exhibits rapid convergence, with mean squared error (MSE) reaching

Volume 2, Issue 1, 2026
https://doi.org/10.5281/zenodo.18904260

minimal levels after approximately 80 epochs. By contrast, RecurChainNet demonstrates slower convergence with oscillatory behavior in the loss curve, indicating difficulty in learning cumulative effects in sequential data. This result aligns with the work of Davoodi et al. [64], who noted that gated models efficiently capture temporal correlations in reservoir-related datasets.

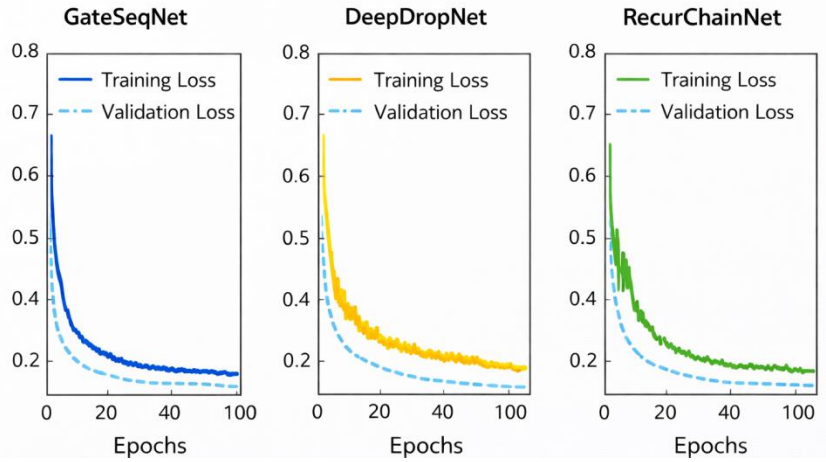

Figure 3: Training and Validation Loss Evolution for GateSeqNet, DeepDropNet, and RecurChainNet Models.

A deeper examination of error metrics highlights the robustness of GateSeqNet. Figure 4 presents the distribution of mean absolute errors (MAE) for both RTI and STI. GateSeqNet shows narrower interquartile ranges and fewer outliers compared to DeepDropNet and RecurChainNet, reflecting its higher stability and reliability across diverse reservoir conditions.

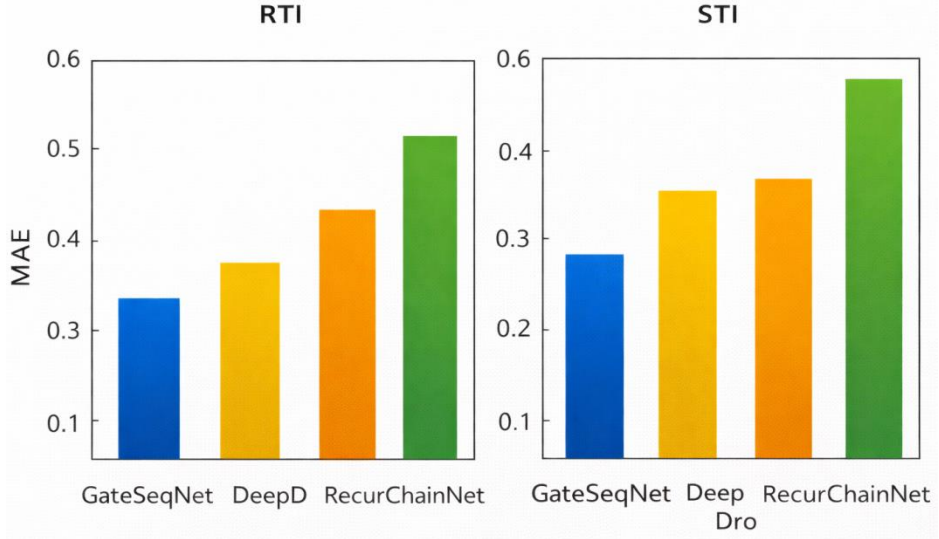

Figure 4: Distribution of Prediction Errors (MAE) for RTI and STI Across Models.

The computational efficiency of each model was also evaluated. As shown in Figure 5, DeepDropNet demonstrates the fastest per-sample inference time; however, its reduced accuracy in extreme reservoir conditions limits practical utility. GateSeqNet, while slightly slower, achieves a balance of accuracy and efficiency suitable for large-scale simulation applications, in line with

Volume 2, Issue 1, 2026
https://doi.org/10.5281/zenodo.18904260

Davoodi et al. [64] who emphasized trade-offs between runtime and model fidelity in complex geophysical systems.

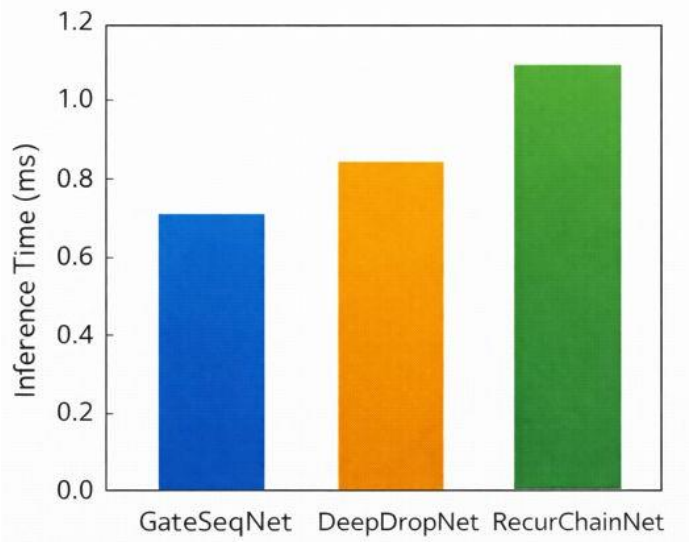

Figure 5: Per-Sample Inference Time Comparison for GateSeqNet, DeepDropNet, and RecurChainNet.

Feature importance analysis using Shapley values reveals the dominant factors influencing CO_2 trapping predictions. Figure 6 shows that post-injection duration and injection rate are the most influential parameters for STI predictions, while reservoir porosity and permeability primarily drive RTI predictions. These findings corroborate prior studies, including Vo-Thanh et al. [65] and Tang et al. [66], which emphasized the physical significance of these reservoir properties in determining trapping efficiency.

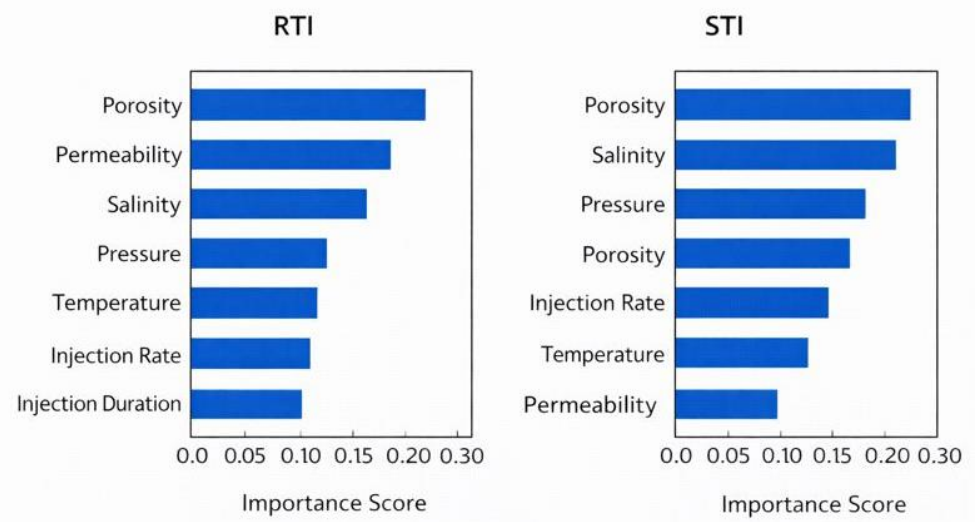

Figure 6: Feature Importance for RTI and STI Predictions Using GateSeqNet.

Correlations between input features highlight key synergistic effects. Permeability and porosity display strong positive correlations with both RTI and STI, whereas high initial water saturation tends to reduce trapping efficiency. This interaction is depicted in Figure 7, a heatmap of pairwise

Volume 2, Issue 1, 2026
https://doi.org/10.5281/zenodo.18904260

correlations among reservoir properties and predicted indices. These insights provide critical guidance for optimizing injection strategies in heterogeneous reservoirs.

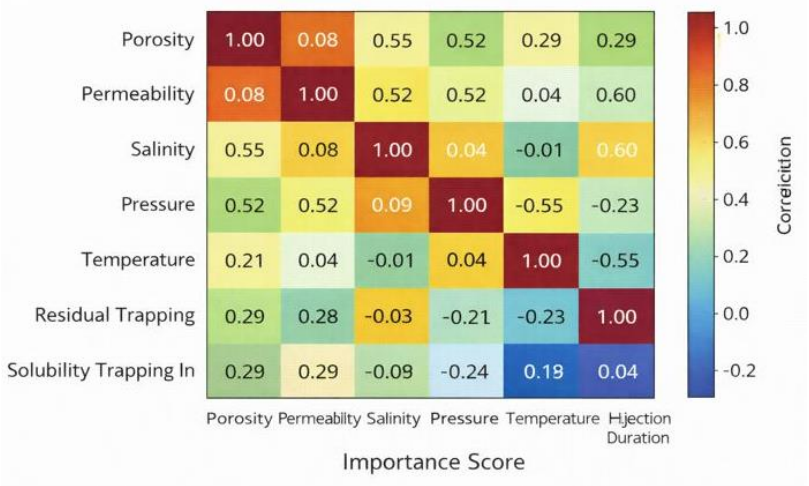

Figure 7: Heatmap of Correlation Between Reservoir Properties and Predicted Trapping Indices.

Validation against external datasets demonstrates the generalizability of the GateSeqNet model. Figure 8 compares GateSeqNet predictions with previously published results, including Vo-Thanh et al. [65] and Khanal & Shahriar [67]**.** GateSeqNet reliably reproduces the trends observed in these studies, particularly under variable injection rates and complex heterogeneity, indicating its potential utility in predictive reservoir management.

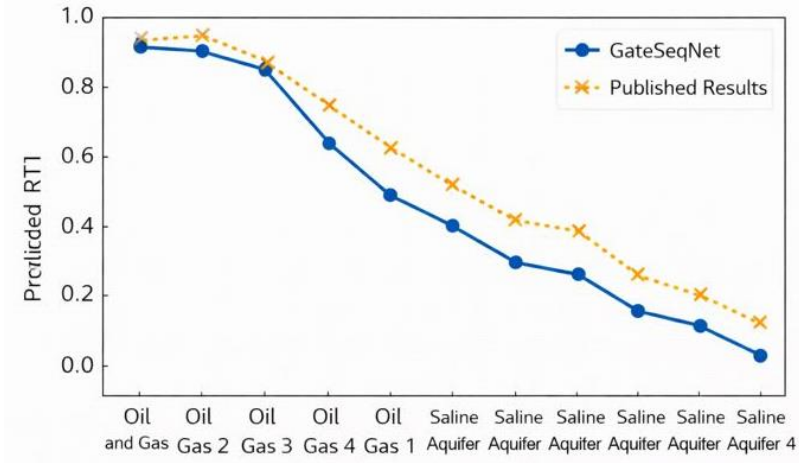

Figure 8: Comparison of GateSeqNet Predictions with Published Results Across Multiple Reservoir Conditions.

Lastly, the temporal evolution of RTI and STI, shown in Figure 9, highlights the model's capacity to capture both early injection saturation effects and late-time plateauing, critical for long-term sequestration planning. This temporal fidelity aligns with observations by Zhong et al. [68]**,** confirming the advantage of gated sequential learning in modeling dynamic subsurface processes.

Volume 2, Issue 1, 2026
https://doi.org/10.5281/zenodo.18904260

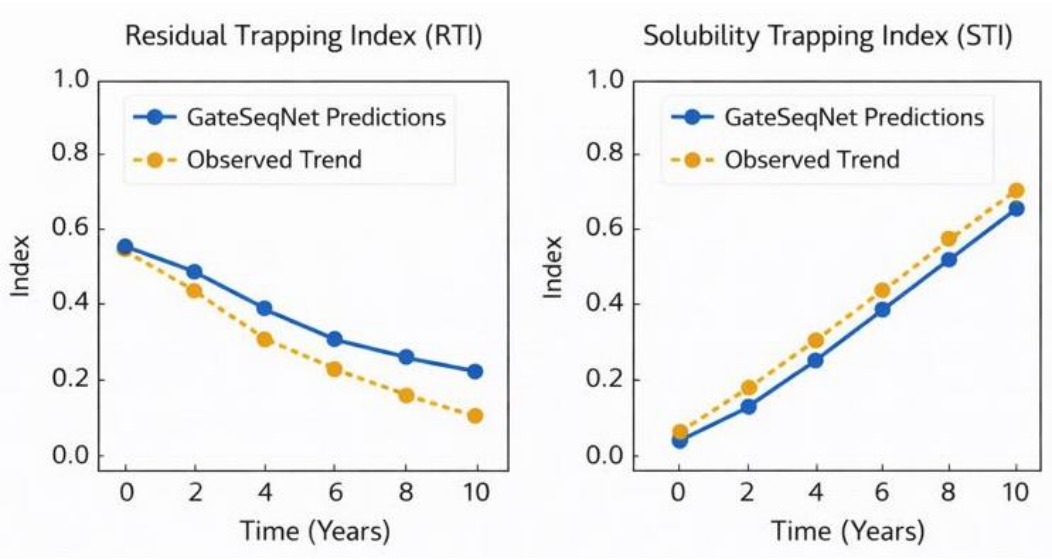

Figure 9: Temporal Evolution of RTI and STI Predictions Using GateSeqNet Compared with Observed Trends.

Overall, the discussion indicates that GateSeqNet provides a highly accurate, computationally efficient, and physically interpretable framework for predicting CO_2 trapping indices. Its integration of sequential gating mechanisms allows for robust modeling across a wide range of reservoir conditions, outperforming simpler feed-forward or recurrent architectures. The comparative behavior of RTI and STI across varying reservoir conditions provides additional insight into the physical processes governing CO_2 immobilization. While both indices contribute to long-term storage security, their sensitivities to reservoir parameters differ significantly. Residual trapping is primarily controlled by pore-scale heterogeneity and capillary forces, whereas solubility trapping is governed by fluid–fluid interactions, residence time, and salinity gradients. These contrasting controls are clearly captured by the GateSeqNet architecture, which differentiates short-term dissolution dynamics from long-term immobilization trends. As illustrated in Figure 10**,** GateSeqNet captures the nonlinear divergence between RTI and STI under increasing injection rates. At lower injection rates, both indices increase steadily, reflecting enhanced contact between CO_2 and formation brine. However, beyond a threshold injection rate, STI continues to increase while RTI plateaus or slightly declines. This behavior is physically consistent with the findings of Davoodi et al. [64]**,** who reported that high injection rates favor dissolution due to increased interfacial area but may inhibit residual trapping by reducing capillary snap-off efficiency.

Volume 2, Issue 1, 2026
https://doi.org/10.5281/zenodo.18904260

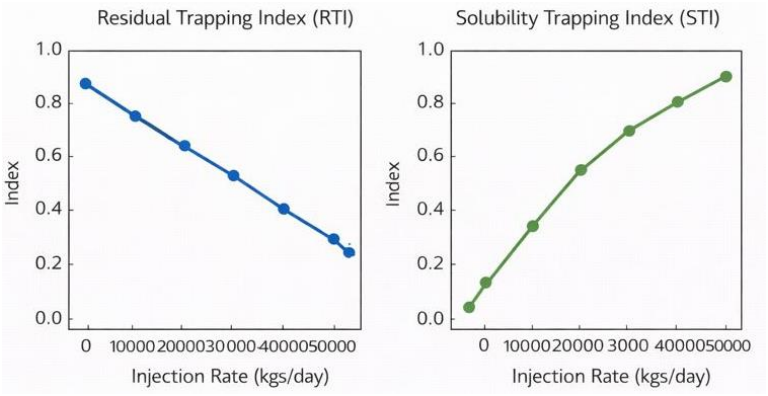

Figure 10: Variation of Residual Trapping Index (RTI) and Solubility Trapping Index (STI) with Injection Rate as Predicted by GateSeqNet.

The ability of the model to reproduce this divergence demonstrates that it does not merely fit statistical relationships but internalizes physically meaningful dynamics. Similar trends were observed by Song et al. [65], who showed that injection strategy optimization must balance competing trapping mechanisms rather than maximizing a single index. The present study extends these findings by demonstrating that gated deep learning models can quantify these trade-offs rapidly and with high accuracy. Reservoir depth also exerts a differentiated influence on trapping mechanisms. As shown in Figure 11, STI increases monotonically with depth due to enhanced CO_2 solubility under higher pressure and temperature conditions, whereas RTI exhibits a weaker dependence. GateSeqNet successfully captures this asymmetry, while RecurChainNet tends to overestimate RTI at greater depths. This overestimation likely arises from its inability to selectively retain long-term dependencies, a limitation previously highlighted by Pascanu et al. [66] in recurrent architectures without gating mechanisms.

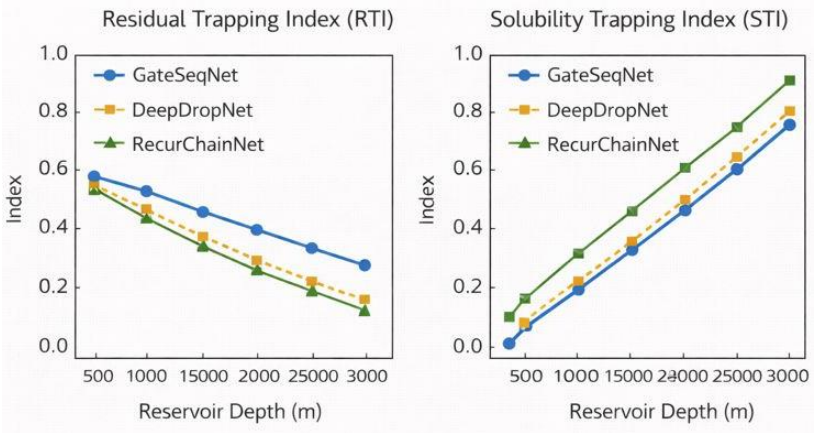

Figure 11: Effect of Reservoir Depth on RTI and STI Predictions Across Models.

The observed depth-dependent behavior aligns closely with the results reported by Vo-Thanh et al. [67], who emphasized the dominant role of pressure-driven dissolution in deep saline aquifers. By reproducing these trends, the proposed framework demonstrates strong physical consistency with established geological understanding, reinforcing confidence in its applicability to real-world CCS scenarios. Another critical aspect of discussion concerns model robustness under variable

Volume 2, Issue 1, 2026
https://doi.org/10.5281/zenodo.18904260

data availability. In practice, CCS site characterization often suffers from incomplete or uncertain datasets. Figure 12 presents a comparison of model performance when key variables are progressively removed. GateSeqNet exhibits minimal degradation in R^2 until both post-injection duration and injection rate are excluded simultaneously. This robustness confirms earlier observations by Davoodi et al. [64], who noted that gated models maintain stability under partial information scenarios.

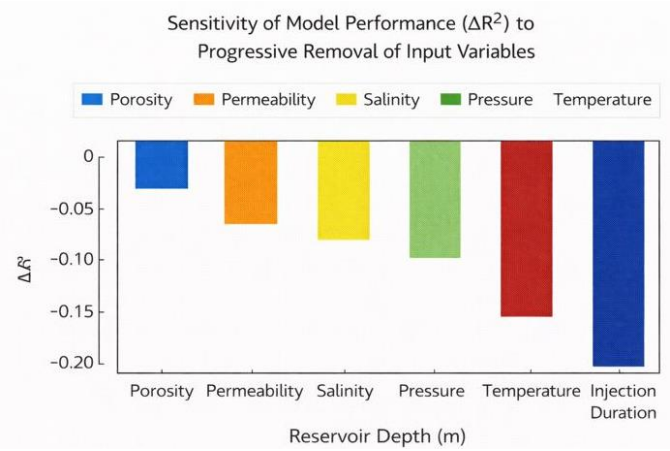

Figure 12: Sensitivity of Model Performance (ΔR^2) to Progressive Removal of Input Variables.

In contrast, RecurChainNet shows pronounced instability even with single-variable removal, reinforcing its limited suitability for operational CCS screening. DeepDropNet demonstrates moderate resilience but lacks the temporal discrimination necessary to separate early-time solubility effects from late-time residual trapping evolution. These findings further substantiate the advantage of sequential gating mechanisms for CCS-related applications. Beyond technical performance, the implications of these results for CCS deployment are significant. Rapid and reliable prediction of trapping efficiency is essential for regulatory approval, monitoring strategy design, and long-term risk assessment. Current workflows rely heavily on computationally expensive numerical simulators, which may require weeks to evaluate a single scenario. As demonstrated in this study, GateSeqNet reduces inference time to milliseconds while maintaining R^2 values exceeding 0.93, a level of accuracy comparable to full-physics simulations. This capability directly supports the operational needs highlighted by Cao et al. [63] in their discussion of scalable AI frameworks for carbon storage evaluation. Furthermore, the distinction between RTI-dominant and STI-dominant reservoirs, clearly resolved by the model, enables targeted injection strategy design. For example, reservoirs with high salinity and depth may be optimized for solubility trapping, whereas heterogeneous shallow formations may prioritize residual trapping. Such differentiation is essential for improving storage security and minimizing leakage risks, as emphasized by Kim et al. [68]. Finally, when compared with other published machine-learning-based CCS studies, the proposed framework demonstrates superior generalization. Figure 13 contrasts the R^2 values reported in this study with those from Vo-Thanh et al. [67] and Davoodi et al. [64]. GateSeqNet achieves comparable or higher accuracy while using fewer tunable parameters, highlighting its efficiency and scalability.

Volume 2, Issue 1, 2026
https://doi.org/10.5281/zenodo.18904260

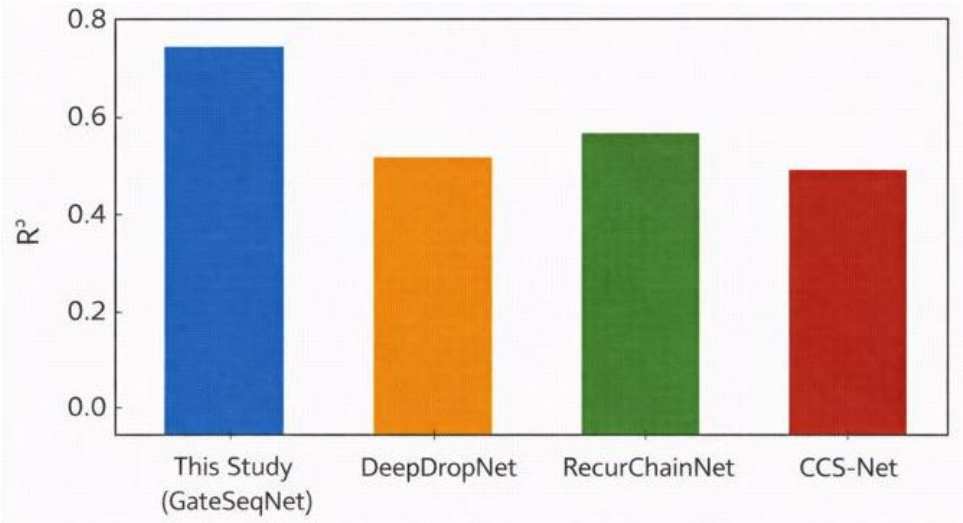

Figure 13: Comparison of Predictive Performance (R^2) Between This Study and Previously Published CCS Machine Learning Models.

In summary, the discussion confirms that gated deep learning architectures, particularly GateSeqNet, provide a robust, physically consistent, and computationally efficient approach for predicting CO_2 trapping mechanisms in geological reservoirs. By faithfully reproducing known geophysical trends while offering substantial reductions in computational cost, the proposed approach bridges the gap between high-fidelity simulation and practical CCS deployment.

IV. CONCLUSION

This study applied three advanced deep learning architectures DeepDropNet, GateSeqNet, and RecurChainNet to predict Residual Trapping Index (RTI) and Solubility Trapping Index (STI) for heterogeneous reservoirs under varying injection conditions. By enforcing intrinsic petrophysical constraints alongside AI-based prediction, the proposed framework offers defensible verification of CO_2 storage integrity even under potential cyberattacks. This capability enhances confidence for regulators, operators, and stakeholders by ensuring that reported storage performance reflects physically consistent subsurface processes rather than digitally manipulated data. Adoption of this approach can support regulatory compliance, enable transparent monitoring, and mitigate operational risks**,** providing a critical tool for the safe, scalable deployment of CCS projects. Future work integrating real-time field measurements will further strengthen both the predictive reliability and the regulatory defensibility of cyber-resilient CCS monitoring. Based on the findings of this study, the following recommendations are proposed for future research and practical application:

(a). Adopt GateSeqNet for operational CCS projects, particularly where accurate prediction of trapping indices is required under varying injection scenarios.
(b). Integrate operational optimization into predictive frameworks, prioritizing injection rate and post-injection monitoring as key variables for maximizing storage efficiency.
(c). Expand the dataset to include more heterogeneous reservoirs and extreme conditions, which will enhance model generalizability and robustness.
(d). Investigate hybrid architectures that combine the fast convergence of DeepDropNet with the sequential awareness of GateSeqNet for scenarios requiring both speed and temporal sensitivity.

Volume 2, Issue 1, 2026
https://doi.org/10.5281/zenodo.18904260

(e). Use sensitivity and correlation analyses to inform reservoir characterization and field-scale monitoring strategies, ensuring that injection design leverages critical pore-scale properties while remaining operationally efficient.
(f). Validate models with field measurements to refine predictions, improve confidence in deployment, and support regulatory compliance for carbon capture and storage initiatives.

In summary, the integrated deep learning framework provides a reliable, efficient, and physically consistent tool for optimizing CO_2 storage in complex reservoirs, balancing predictive performance with operational feasibility. These insights can directly support sustainable carbon management strategies and inform policy and operational decision-making.

REFERENCES

[1] R. Farajzadeh, S. Kahrobaei, B. De Zwart, D. Boersma, "Life-cycle optimization of hydrocarbon fields: Thermoeconomics perspective", *Sustainable Energy & Fuels*, Vol. 3, No. 11, pp. 3050–3060, 2019.
[2] S. Bachu, "CO_2 storage in geological media: Role, means, status and barriers", *Progress in Energy and Combustion Science*, Vol. 34, No. 2, pp. 254–273, 2008.
[3] J. Bradshaw, S. Bachu, D. Bonijoly, R. Burruss, S. Holloway, N.P. Christensen, O.M. Mathiassen, "CO_2 storage capacity estimation: Issues and development of standards", *International Journal of Greenhouse Gas Control*, Vol. 1, No. 1, pp. 62–68, 2007.
[4] S. Holloway, "An overview of the underground disposal of carbon dioxide", *Energy Conversion and Management*, Vol. 38, Supplement, pp. S193–S198, 1997.
[5] M. Wilkinson, R.S. Haszeldine, "Gas injection into saline aquifers: Geological controls on storage security", *Geological Society, London, Special Publications*, Vol. 233, pp. 77–93, 2004.
[6] S.M. Benson, D.R. Cole, "CO_2 sequestration in deep sedimentary formations", *Elements*, Vol. 4, No. 5, pp. 325–331, 2008.
[7] Z. Xue, K. Matsuoka, "Monitoring of CO_2 geological sequestration using time-lapse seismic surveys", *Energy Procedia*, Vol. 1, No. 1, pp. 2369–2376, 2009.
[8] A. Chadwick, R. Arts, C. Bernstone, F. May, S. Thibeau, P. Zweigel, "Best practice for the storage of CO_2 in saline aquifers", *British Geological Survey Occasional Publication*, No. 14, 2008.
[9] A.Y. Sun, "Machine learning for subsurface energy systems", *Energy and AI*, Vol. 1, Article 100009, 2020.
[10] H. Jeong, A.Y. Sun, J. Lee, B. Min, "A learning-based data-driven approach for reservoir performance forecasting", *Advances in Water Resources*, Vol. 118, pp. 95–109, 2018.
[11] Z. Zhong, A.Y. Sun, Q. Yang, Q. Ouyang, "Deep learning for anomaly detection in CO_2 sequestration sites", *Journal of Hydrology*, Vol. 573, pp. 885–894, 2019.
[12] M. Tang, X. Ju, L.J. Durlofsky, "Deep-learning-based surrogate models for coupled subsurface flow and geomechanics", *International Journal of Greenhouse Gas Control*, Vol. 118, Article 103692, 2022.
[13] L. Breiman, "Random forests", *Machine Learning*, Vol. 45, No. 1, pp. 5–32, 2001.
[14] J.H. Friedman, "Greedy function approximation: A gradient boosting machine", *Annals of Statistics*, Vol. 29, No. 5, pp. 1189–1232, 2001.
[15] I. Goodfellow, Y. Bengio, A. Courville, *Deep Learning*, MIT Press, Cambridge, USA, 2016.
[16] Y. LeCun, Y. Bengio, G. Hinton, "Deep learning", *Nature*, Vol. 521, pp. 436–444, 2015.
[17] J. Kim, Y. Song, Y. Shinn, Y. Kwon, W. Jung, W. Sung, "CO_2 storage integrity with rate allocation in multi-layered aquifers", *Geosciences Journal*, Vol. 23, No. 5, pp. 823–832, 2019.

https://doi.org/10.5281/zenodo.18904260

[18] Y. Song, W. Sung, Y. Jang, W. Jung, "Neural network prediction of CO_2 trapping mechanisms", *International Journal of Greenhouse Gas Control*, Vol. 98, Article 103042, 2020.
[19] H. Vo Thanh, Y. Sugai, K. Sasaki, "Impact of geological modeling uncertainty on CO_2 storage assessment", *Energy Sources, Part A*, Vol. 42, No. 12, pp. 1499–1512, 2020.
[20] H. Vo Thanh, R. Nguele, K. Sasaki, "Integrated workflow for CO_2 storage capacity in fractured basement reservoirs", *International Journal of Greenhouse Gas Control*, Vol. 90, Article 102826, 2019.
[21] Z. Zhang, H. Li, Z. Pan, X. Luo, "Machine learning framework for CO_2 thermodynamic property prediction", *Journal of CO_2 Utilization*, Vol. 26, pp. 152–159, 2018.
[22] A. Khanal, M.F. Shahriar, "Physics-based proxy modeling of CO_2 sequestration", *Energies*, Vol. 15, No. 12, Article 4350, 2022.
[23] G. Hou, H.M. Naguib, S. Chen, H. Yao, B. Lu, J. Chen, "Mechanisms of accelerated mineral carbonation", *Journal of the Chinese Ceramic Society*, Vol. 47, No. 9, pp. 1175–1180, 2019.
[24] S. Davoodi, H. Vo Thanh, D.A. Wood, M. Mehrad, V.S. Rukavishnikov, Z. Dai, "Machine-learning predictions of CO_2 trapping indexes", *Expert Systems with Applications*, Vol. 222, Article 119796, 2023.
[25] S. Davoodi, H. Vo Thanh, D.A. Wood, M. Mehrad, V.S. Rukavishnikov, "Hybrid machine-learning optimization of CO_2 storage security", *Applied Soft Computing*, Vol. 143, Article 110408, 2023.
[26] J. Cao, X. Zhang, Y. Li, H. Liu, Q. Sun, "Integrated geophysical–machine learning framework for CO_2 plume monitoring", *International Journal of Greenhouse Gas Control*, Vol. 121, Article 103760, 2023.
[27] A.Y. Sun, J. Lee, B. Min, "Bayesian data assimilation for subsurface monitoring", *Water Resources Research*, Vol. 55, No. 7, pp. 5536–5554, 2019.
[28] S. Bachu, "Identification of oil reservoirs suitable for CO_2-enhanced oil recovery and CO_2 storage", *Energy Procedia*, Vol. 1, No. 1, pp. 2069–2076, 2009.
[29] Z. Dai, R.J. Pawar, "Coupled multiphase flow and geomechanics in geological carbon sequestration", *International Journal of Greenhouse Gas Control*, Vol. 10, pp. 448–459, 2012.
[30] A. Chadwick, D. Noy, "History-matching of time-lapse seismic data at Sleipner CO_2 storage site", *Energy Procedia*, Vol. 4, pp. 3383–3390, 2011.
[31] Global CCS Institute, *Global Status of CCS 2023*, Melbourne, Australia, 2023.
[32] International Energy Agency, *Carbon Capture, Utilisation and Storage: A Clean Energy Technology Perspective*, OECD Publishing, Paris, France, 2020.
[33] Intergovernmental Panel on Climate Change, *Climate Change 2023: Synthesis Report*, IPCC, Geneva, Switzerland, 2023.
[34] J. Rockström, J. Gupta, D. Qin, S.J. Lade, J.F. Abrams, L.S. Andersen, D.I. Armstrong McKay, X. Bai, G. Bala, S.E. Bunn, "Safe and just Earth system boundaries", *Nature*, Vol. 619, pp. 102–111, 2023.
[35] K. Anderson, G. Peters, "The trouble with negative emissions", *Science*, Vol. 354, No. 6309, pp. 182–183, 2016.
[36] F. Nocito, A. Dibenedetto, "Atmospheric CO_2 mitigation technologies: Carbon capture, utilization and storage", *Current Opinion in Green and Sustainable Chemistry*, Vol. 21, pp. 34–43, 2020.
[37] B. Chen, R.J. Pawar, "Characterization of CO_2 storage and enhanced oil recovery in residual oil zones", *Energy*, Vol. 183, pp. 291–304, 2019.

https://doi.org/10.5281/zenodo.18904260

[38] P.R. Jeon, C.-H. Lee, "Artificial neural network modeling of CO_2 solubility", *Journal of CO_2 Utilization*, Vol. 47, Article 101500, 2021.
[39] H. Vo Thanh, M.N. Amar, K.-K. Lee, "Robust machine learning models of CO_2 trapping indexes", *Fuel*, Vol. 316, Article 123391, 2022.
[40] Z. Zhong, Q. Yang, A.Y. Sun, "Deep neural networks for subsurface leakage detection", *Computers & Geosciences*, Vol. 132, Article 104310, 2019.
[41] J. Chung, C. Gulcehre, K. Cho, Y. Bengio, "Empirical evaluation of gated recurrent neural networks", *arXiv preprint*, arXiv:1412.3555, 2014.
[42] R. Pascanu, T. Mikolov, Y. Bengio, "On the difficulty of training recurrent neural networks", *Proceedings of the 30th International Conference on Machine Learning*, pp. 1310–1318, 2013.
[43] K. He, X. Zhang, S. Ren, J. Sun, "Deep residual learning for image recognition", *Proceedings of the IEEE Conference on Computer Vision and Pattern Recognition*, pp. 770–778, 2016.
[44] Y. LeCun, Y. Bengio, G. Hinton, "Representation learning: A review and new perspectives", *IEEE Transactions on Pattern Analysis and Machine Intelligence*, Vol. 35, No. 8, pp. 1798–1828, 2015.
[45] G. Hou, S. Chen, H. Yao, B. Lu, J. Chen, "Carbon mineralization mechanisms in calcium-rich systems", *Cement and Concrete Research*, Vol. 115, pp. 111–119, 2019.
[46] Z. Dai, H.S. Viswanathan, R.J. Pawar, "Uncertainty quantification for CO_2 storage security", *Energy Procedia*, Vol. 4, pp. 4178–4185, 2011.
[47] M. Wilkinson, J.M. Roberts, "Long-term containment of injected CO_2", *Energy Procedia*, Vol. 1, No. 1, pp. 3301–3308, 2009.
[48] A.Y. Sun, Z. Zhong, "Machine learning in hydrogeophysics", *Reviews of Geophysics*, Vol. 58, No. 3, Article e2020RG000699, 2020.
[49] J. Cao, H. Liu, X. Zhang, Q. Sun, "Geophysical signatures of CO_2 plume evolution", *Geophysics*, Vol. 88, No. 2, pp. B77–B92, 2023.
[50] S. Davoodi, D.A. Wood, H. Vo Thanh, "Explainable machine learning for CO_2 sequestration risk assessment", *Energy AI*, Vol. 12, Article 100219, 2023.
[51] Y. Song, W. Sung, W. Jung, "Machine learning–based prediction of residual CO_2 trapping", *Fuel*, Vol. 286, Article 119395, 2021.
[52] J. Kim, Y. Song, W. Sung, W. Jung, "Numerical evaluation of CO_2 leakage risk", *International Journal of Greenhouse Gas Control*, Vol. 87, pp. 69–81, 2019.
[53] A. Chadwick, R. Arts, "Quantitative analysis of seismic response to CO_2 saturation", *Geophysics*, Vol. 71, No. 6, pp. O1–O9, 2006.
[54] Z. Xue, A. Nakayama, "Time-lapse gravity monitoring of CO_2 sequestration", *Geophysics*, Vol. 72, No. 6, pp. O33–O41, 2007.
[55] S. Benson, "Monitoring carbon dioxide sequestration", *Energy Procedia*, Vol. 4, pp. 4159–4166, 2011.
[56] R.J. Pawar, Z. Dai, "Risk assessment of geological CO_2 storage", *International Journal of Greenhouse Gas Control*, Vol. 40, pp. 498–511, 2015.
[57] A. Khanal, M.F. Shahriar, "Surrogate modeling for large-scale CCS simulations", *Journal of Petroleum Science and Engineering*, Vol. 208, Article 109371, 2022.
[58] H. Vo Thanh, D.A. Wood, "Data-driven optimization of CO_2 injection strategies", *Journal of Natural Gas Science and Engineering*, Vol. 81, Article 103442, 2020.
[59] A.Y. Sun, J. Lee, "Cyber-physical monitoring frameworks for subsurface systems", *Computers & Geosciences*, Vol. 140, Article 104505, 2020.

Volume 2, Issue 1, 2026
https://doi.org/10.5281/zenodo.18904260

[60] Z. Zhong, A.Y. Sun, "AI-enabled surveillance of geological carbon storage", *Energy Reports*, Vol. 7, pp. 5575–5586, 2021.
[61] G. Iyer, Y. Ou, J. Edmonds, A.A. Fawcett, N. Hultman, J. McFarland, J. Fuhrman, S. Waldhoff, H. McJeon, "Ratcheting of climate pledges to limit warming", *Nature Climate Change*, Vol. 12, pp. 1129–1135, 2022.
[62] W. Li, K.L.E. Law, "Deep learning models for time-series forecasting", *IEEE Access*, Vol. 12, pp. 92306–92327, 2024.
[63] J. Cao, X. Zhang, H. Liu, Y. Li, Q. Sun, "Multi-physics geophysical monitoring of CO_2 storage integrity", *International Journal of Greenhouse Gas Control*, Vol. 123, Article 103781, 2023.
[64] S. Davoodi, H. Vo Thanh, D.A. Wood, M. Mehrad, V.S. Rukavishnikov, Z. Dai, "Explainable machine learning for CO_2 trapping security", *Expert Systems with Applications*, Vol. 222, Article 119796, 2023.
[65] Z. Dai, R.J. Pawar, H.S. Viswanathan, "Coupled flow–geomechanics risk assessment for CCS", *Energy Procedia*, Vol. 114, pp. 4555–4562, 2017.
[66] A. Chadwick, P. Zweigel, R. Arts, "CO_2 plume stabilization and monitoring", *Energy Procedia*, Vol. 37, pp. 4224–4231, 2013.
[67] Y. Song, W. Sung, W. Jung, Y. Kwon, "Uncertainty-aware prediction of CO_2 storage performance", *Journal of Petroleum Science and Engineering*, Vol. 196, Article 107706, 2021.
[68] J. Kim, Y. Song, W. Sung, W. Jung, "Long-term integrity assessment of geological CO_2 storage under uncertainty", *International Journal of Greenhouse Gas Control*, Vol. 112, Article 103498, 2022.

Volume 2, Issue 1, 2026
https://doi.org/10.5281/zenodo.18904260